

# Simulation of One-Port SAW Resonator using COMSOL Multiphysics

Rama Krishnan N.<sup>1</sup>, Harshal B. Nemade<sup>\*1,2</sup>, Roy Paily<sup>2</sup>

<sup>1</sup>Center for Nanotechnology, Indian Institute of Technology, Guwahati

<sup>2</sup>Department of Electronics and Communication Engineering, Indian Institute of Technology, Guwahati

\*Corresponding author: Centre for Nanotechnology, Indian Institute of Technology Guwahati, Guwahati 781039, India, harshal@iitg.ernet.in

**Abstract:** In this paper, we discuss simulation of one-port surface acoustic wave (SAW) resonators using COMSOL Multiphysics. SAW devices are widely used in electronic systems in the recent years. SAW is a mechanical wave excited by interdigital transducer (IDT) fabricated over a piezo crystal. IDT has a comb-like structure, where the distance between the fingers in the IDT decides the frequency of the wave propagating over the substrate. Resonator action can be achieved in one of the two ways; a single IDT having several fingers over a piezoelectric substrate or a short IDT with reflecting gratings at the ends of the IDT. We have modeled a Rayleigh wave type SAW device choosing YZ Lithium Niobate as the substrate and aluminum metal electrodes as IDT. Considering the computation time for simulating the total SAW device, a section of the SAW Resonator is modeled and the results are validated for the full device. We would like to show SAW resonator as a typical example for simulating SAW devices using COMSOL Multiphysics.

**Keywords:** MEMS, SAW devices, Resonators, IDT.

## 1. Introduction

Surface acoustic waves (SAWs) are ultrasonic waves propagating along the surface of solids. An interdigital transducer (IDT) performs the function of conversion of electrical energy to mechanical energy and vice versa. IDT is a comb-shaped structure fabricated over the piezoelectric substrate. A voltage applied to the IDT produces dynamic strains in the substrate and initiates elastic waves that travel along the surface. Various types of SAW devices based on Rayleigh wave, SH-SAW, Love wave, acoustic plate mode (APM), flexural plate wave (FPM) have been explored for sensors and telecommunication applications [2] [3]. The propagation of acoustic waves in piezoelectric

media depends on the substrate material properties, the crystal cut, and the structure of the electrodes. The distance  $p$  between successive electrodes as shown in Figure 1 decides the elastic wavelength  $\lambda$  and they are related by

$$\lambda = 2p \quad (1)$$

The associated frequency  $f$  of the waves propagating with velocity  $v$  is given by

$$f = v/\lambda \quad (2)$$

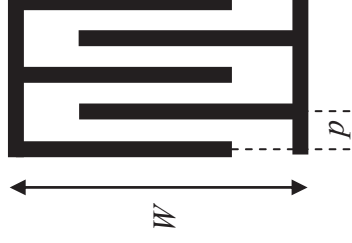
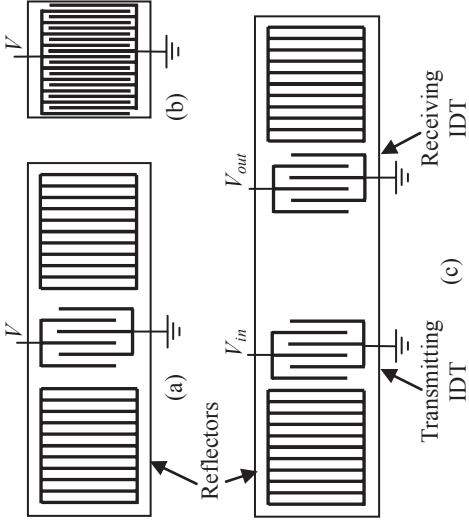


Figure 1. Interdigital transducer (IDT).

A typical SAW device in sensor applications consists of a transmitting IDT and a receiving IDT separated by a few wavelengths that forms the delay line model. IDTs along with reflectors find more application in telecommunication circuits like resonators, filters, convolvers. Resonators are also used for sensor applications [6].

## 2. SAW Resonators

SAW resonators are mainly classified into two types: one-port and two-port resonators as shown in Figure 2. One-port resonator action can be achieved by multiple reflections between the fingers of a long IDT or reflections by the reflectors at the either end of a short IDT. SAW resonators simulation using COM model has been reported by Wu et al [7]. FEM simulation using periodic and absorbing boundaries is



**Figure 2.** (a) & (b) One-port SAW resonators, (c) Two-port SAW resonator.

reported by Hofer et al [1] [9]. Kannan [5] demonstrated SAW resonator using ANSYS. To the best of our knowledge modeling of SAW resonator using COMSOL Multiphysics is demonstrated for the first time in this paper.

The Rayleigh elastic wave displacement has components in surface-normal and surface-parallel directions with respect to the direction of the wave propagation. The particle in the upper surface takes elliptical path having both the components.

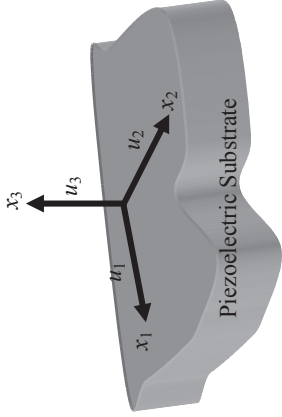


**Figure 3.** Coordinate system for the wave solutions.

The displacement of the surface  $u_1$ ,  $u_2$ ,  $u_3$  along  $x_1$ ,  $x_2$ ,  $x_3$  directions for Rayleigh wave as shown in Figure 3 is given by equations (3–5).

$$u_1 = [A_1 \exp(-b_1 x_3) + A_2 \exp(-b_2 x_3)] \exp(jk(x_1 - ct)) \quad (3)$$

$$u_2 = 0 \quad (4)$$

$$u_3 = [(-b_1/jk)A_1 \exp(-b_1 x_3) + (jk/b_2)A_2 \exp(-b_2 x_3)] \exp(jk(x_1 - ct)) \quad (5)$$

where  $A_1$ ,  $A_2$  are amplitudes, and

$$b_1 = k(1 - c^2/v_t^2)^{1/2}$$

$$b_2 = k(1 - c^2/v_l^2)^{1/2}$$

$v_l$  and  $v_t$  are longitudinal and transverse wave velocities,  $k$  is the wave number,  $c$  is the velocity of SAW.

#### 4. Simulation Settings

All FEM simulations are performed using COMSOL Multiphysics 3.2 in a Pentium 4HT(IBM) Machine.

##### 4.1 Geometry settings

Since  $x_2$  does not contain much information of Rayleigh SAW, we can consider the total device as a small section as in the Figure 4. The intensity of the SAW is confined more within  $1 \lambda$  thickness of the substrate [3]. The IDTs are periodic in nature consisting of positive and negative potentials alternately, thus one electrode is sufficient to model the SAW resonator as a whole. In this simulation we have analyzed structures with one electrode and two electrodes over piezoelectric substrate. The geometry is drawn in 2D and extruded to 3D.

##### 4.2 Subdomain settings

Lithium Niobate piezoelectric crystal is used as the substrate. The elastic constants, permittivity constants, stress constants are taken from [10] and  $Y$  cut  $Z$  propagating constants are provide as in Appendix. Aluminum is chosen for electrode with Poisson ratio, density, Young's modulus as in Appendix.

##### 4.3 Boundary settings

The geometry of the SAW structure used in the simulation is given in Table 1. Traction free boundary is given to the top surface of the substrate. The Bottom surface is fixed in its position and the displacement in the lateral direction is constrained to zero. As the IDTs are periodic in nature, appropriate periodic boundary conditions are applied using the equations (6–8) [1] [9] [4].

**Table 1:** Dimensions of IDT and substrate

Aluminum electrode thickness	200 nm
Periodicity of the electrode ( $p$ )	4 $\mu\text{m}$
Width of the electrode	1 $\mu\text{m}$
Aperture ( $W$ )	0.5 $\mu\text{m}$ , 0.25 $\mu\text{m}$ , 0.125 $\mu\text{m}$
Substrate thickness	4 $\mu\text{m}$ ( $1 \lambda$ )

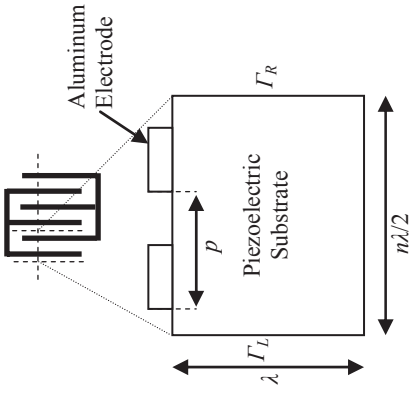


Figure 4. Geometry employed in the simulation.

$$u_i(x+np) = u_i(x) \exp(-j2\pi\gamma n) \quad (6)$$

$$V_i(x+np) = V_i(x) \exp(-j2\pi\gamma n) \quad (7)$$

$$\Gamma_R(u, V) = \rho \Gamma_L(u, V) \quad (8)$$

where  $\rho = (-1)^n$ ,  $\gamma$  is complex proration constant,  $u_i$  is the displacement,  $V_i$  is the potential. A potential of 10 V is applied to the electrodes in the simulation.

## 5. Results and Discussions

Figures (5) and (6) show the simulated deformed displacement along the Y-direction and X-direction of one-port SAW resonator, respectively for two electrode structure. The displacement profile shows the Rayleigh wave propagation over the substrate with amplitude of 17 nm. The accuracy depends on the mesh employed. With a base mesh of 336 elements extended to a mesh of 14400 degrees of freedom, we obtained a Rayleigh wave with a velocity of 3552 m/s at a synchronous frequency of 888 MHz, consistent with the results produced by Kannan [5]. In order to have better accuracy only single electrode is simulated with refined mesh having 27500 degrees of freedom. As a result, the wave velocity of 3488 m/s is observed, which is more accurate velocity of Rayleigh wave for YZ-Lithium Niobate substrate at synchronous frequency of 871 MHz [11]. From frequency response analysis, complex charge  $Q$  (or current in the electrode) is extracted from post processing, thus the admittance ( $Y$ ) of the device can be calculated by equation

$$Y = j\omega Q/V_i \quad (9)$$

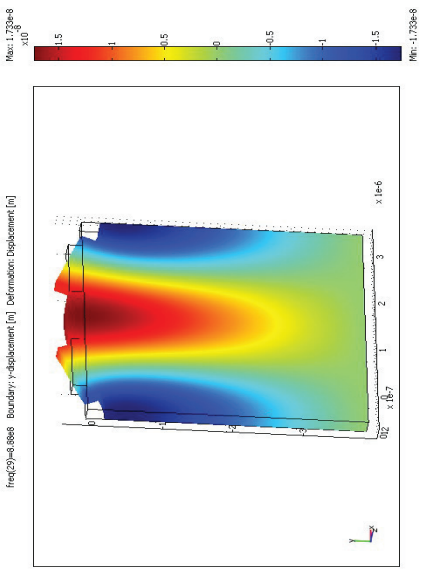


Figure 5: Deformed Y-displacement.

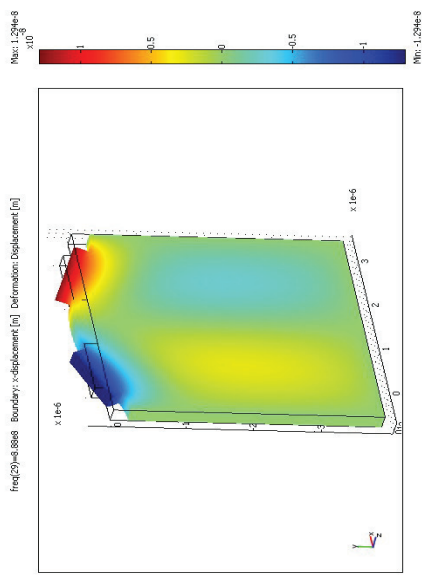


Figure 6: Deformed X-displacement.

The aperture length of IDT is denoted by  $W$  as in Figure 1. Admittance versus frequency plots for an aperture  $W$  of 0.5  $\mu\text{m}$ , 0.25  $\mu\text{m}$ , and 0.125  $\mu\text{m}$  are shown in Figure 7. The admittance values at 871 MHz are  $6.3 \times 10^{-5}$  mho,  $2.78 \times 10^{-5}$  mho,  $1.365 \times 10^{-5}$  mho, respectively. Accordingly total IDT admittance for fixed aperture is an integral multiple of the reduced model. As an extension of the model, a delay line SAW device is simulated and the pattern of Rayleigh wave propagation with respect to time is shown in Figure 8 where proper absorbing boundaries are applied in the ends of the SAW device.

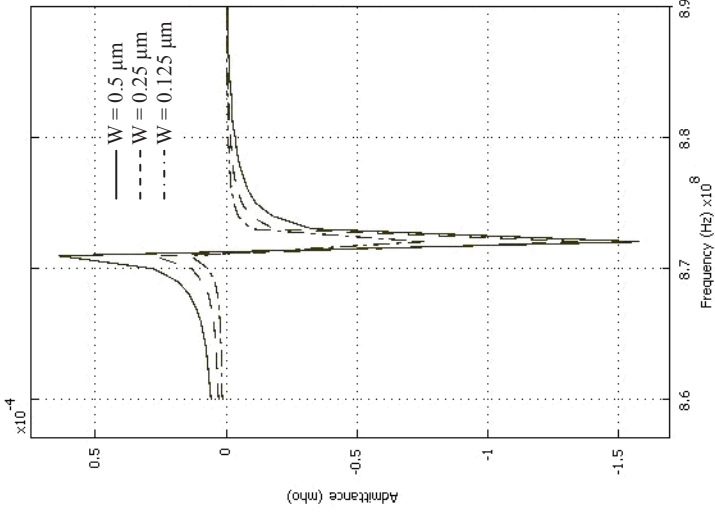


Figure 7. Frequency response of YZ-Lithium Niobate.

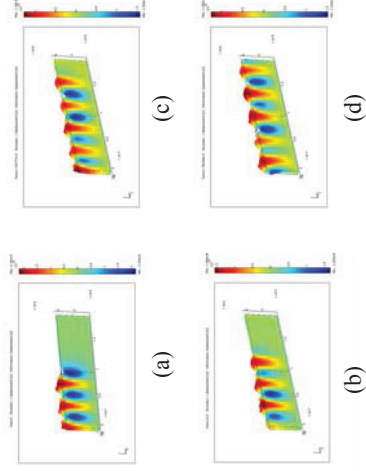


Figure 8: Sequence of wave traveling over the substrate (time domain analysis).

## 6. Conclusions

A one-port SAW resonator is simulated by using COMSOL Multiphysics. The results are summarized for typical mesh parameters. It is shown that COMSOL Multiphysics can be used to simulate SAW devices. The delay line model can be further used for simulating SAW sensors.

## 7. References

1. M. Hofer, N. Finger, G. Kovacs, J. Schoberl, S. Zaglmayr, U. Langer, and R. Lerch, Finite-element simulation of wave propagation in periodic piezoelectric SAW structures, *IEEE*

*Transactions on Ultrasonics, Ferroelectrics, and Frequency Control*, **53**, 1192–1201 (2006)

2. D. S. Ballantine, R. M. White, S. I. Martin, A. I. Ricco, E. T. Zellers, G. C. Frye, H. Wohltjen, *Acoustic Waves Sensors Theory, Design, and Physico-Chemical Applications*. Academic Press (1997)
3. J. W. Gardner, V. K. Vardhan, O. O. Awadelkarim, *Microsensors, MEMS, and Smart Devices*, 303–416. John Wiley & Sons, England (2001)
4. *COMSOL Multiphysics Users Guide*, Ver 3.2 (2005)
5. T. Kannan, Finite Element Analysis of Surface Acoustic Wave Resonators, *Master Thesis*, University of Saskatchewan, (2006)
6. T. Nomura, M. Tekebayashi, A. Saitoh, Chemical sensor based on surface acoustic resonator using Langmuir-Blodgett film, *IEEE Transactions on Ultrasonics, Ferroelectrics, and Frequency Control*, **45**, 1261–1265 (1998)
7. T. T. Wu, S. M. Wang, Y. Y. Chen, T. Y. Wu, P. Z. Chang, L. S. Huang, C. L. Wang, C. W. Wu, and C. K. Lee, Inversion determination of coupling of modes parameters of surface acoustic wave resonators, *Jpn. J. Appl. Phys.*, **41**, 6610–6615 (2002).
8. H. Subramanian, V. K. Vardan, V. V. Vardan, M. J. Vellekoop, Design and fabrication of wirelessly remotely readable MEMS based microaccelerometers, *Smart Mater. Struct.*, **6**, 730–738 (1997)
9. M. Hofer, N. Finger, G. Kovacs, J. Schoberl, U. Langer, and R. Lerch, Finite-element simulation of bulk and surface acoustic wave (SAW) interaction in SAW devices, *IEEE Ultrasonics Symposium* (2002)
10. A. W. Warner, M. Onoe, and G. A. Coquin, Determination of elastic and piezoelectric constants for crystals in class (3M), *Acoustical Society of America* (1968).
11. E. L. Adler, Bulk and surface acoustic waves in anisotropic solids, *International Journal of High Speed Electronics and Systems*, **10**, 653–684 (2000)

## 8. Appendix

### 8.1 YZ-Lithium Niobate constants

Density: 4650 kg/m<sup>3</sup>

Elastic constants ( $C_{ij}^E$ ):

$$\begin{bmatrix} 2.45 & 0.75 & 0.75 & 0 & 0 & 0 \\ 0.75 & 2.03 & 0.53 & 0 & 0.09 & 0 \\ 0.75 & 0.53 & 2.03 & 0 & -0.09 & 0 \\ 0 & 0 & 0 & 0.75 & 0 & 0.09 \\ 0 & 0.09 & -0.09 & 0 & 0.60 & 0 \\ 0 & 0 & 0 & 0.09 & 0 & 0.60 \end{bmatrix} \times 10^{11} \text{ N/m}^2$$

Permittivity constants ( $\epsilon$ ):

$$\begin{bmatrix} 1.3 & 0.2 & 0.2 & 0 & 0 & 0 \\ 0 & 0 & 0 & -2.5 & 0 & 3.7 \\ 0 & -2.5 & 2.5 & 0 & 3.7 & 0 \end{bmatrix} \text{ C/m}^2$$

Relative dielectric constants ( $\epsilon_{ij}^S$ ):

$$\begin{bmatrix} 29 & 0 & 0 \\ 0 & 44 & 0 \\ 0 & 0 & 44 \end{bmatrix}$$

### 8.2 Aluminium constants

Young's modulus: 70 GPa

Poisson ratio: 0.35

Density: 2700 kg/m<sup>3</sup>